Investigations for CFD Based Form Factor Methods

Investigations for CFD Based Form Factor Methods

Kadir Burak Korkmaz[*] [†], **Sofia Werner**[†], **and Rickard Bensow**[*]
[*]Chalmers University of Technology, Gothenburg/Sweden, [†]SSPA Sweden AB, Gothenburg/Sweden
korkmaz@chalmers.se

1 Introduction

Performance prediction of full-scale ship is one of the most important tasks in the design stage. Depending on the design phase, required accuracy of the prediction varies as well as the prediction methods. Often towing tank tests are carried out at the last stage of the design process. The procedures of the towing tank tests are regulated by the International Towing Tank Committee (ITTC) and the prediction is based on the 1978 ITTC Performance Prediction Method. The form factor concept was adopted by this method as described by Hughes (1954), where the viscous resistance is expressed in relation to the 'ITTC 57 model-ship correlation line' as shown in the Eq. (1).

$$C_V = (1 + k)\, C_F. \tag{1}$$

The concept of Hughes (1954) and the determination method of Prohaska (1966) of form factor have been questioned and investigated for many decades. By analyzing the geosim test data, García-Gómez (2000), Toki (2008) and Van et al. (2011) demonstrated the scale effects on form factor. Additionally, CFD studies presented by Raven et al. (2009) and Wang et al. (2015) supported the existence of substantial scale effects on form factor. The main cause of the scale effects has been found to be the 'ITTC 57 model-ship correlation line' rather than the original hypothesis of Hughes (1954) which suggested that form factor is independent of the Reynolds number. As explained by Raven et al. (2009), scale effects on the form factor depends on several aspects:

1. The assumption that the form factor is not dependent on the Reynolds number. As Raven et al. (2009) and Wang et al. (2015) presented, viscous resistance was nearly proportional for bare hull when modern friction lines, i.e. Grigson (1999) and Katsui (2005), or numerical friction of the same turbulence model is used for extrapolation.

2. The friction line used for the extrapolation method

3. If form factor is determined by CFD, choice of turbulence model might play a significant role

Additionally, when the growing disposition to leave the Prohaska's method of form factor determination and growing confidence in numerical resistance calculations considered, CFD might be able to provide a new method of form factor determination, which can increase the accuracy of the full-scale resistance predictions.

In this study, the form factor concept has been investigated by analyzing the results obtained from the simulations performed on KVLCC2 and KCS hulls. Grid dependence studies, sensitivity analysis of loading conditions and varying grid setups have been performed with SHIPFLOW code. Extrapolation of viscous resistance to full scale has been performed with ITTC57 line and numerical friction lines.

2 Flow Solver, Computational Domain, Grid Generation

Two of the flow solvers and the structured grid generator of SHIPFLOW 6.3 has been used for this study. Potential flow solver, XPAN, is used for obtaining sinkage and trim for the bare hull. Viscous flow is solved with the XCHAP module which solves the Reynolds Averaged Navier-Stokes equations with a finite volume method. XCHAP is a steady state solver which requires structured grids but overlapping grids can be used to introduce refinement regions or appendages.

Viscous flow computations for all cases were carried as double model. The computational domain consists of six boundaries. The distance between inlet and fore-perpendicular (FP) is $0.5L_{PP}$. Outlet plane is located at $0.8L_{PP}$ behind the aft-perpendicular and the radius of the cylindrical outer boundary is $3L_{PP}$ in order to eliminate the blockage effect as much as possible. EASM and $k-\omega$ SST turbulence

models have been used for this study. All simulations performed as wall resolved, i.e. no wall functions used. The computational conditions are presented in Table 1.

Table 1: Computational conditions for the KVLCC2 and KCS hulls

Ship	L (m)	Scale	T (m)	S/L^2	Speed	Rn model	Rn ship	Vm (m/s)	Vs (kts)
KLVCC2 with rudder	320	58	20.8	0.2682	Low	4.1×10^6	1.80×10^9	0.88	13
					Design	4.9×10^6	2.14×10^9	1.05	15.5
KCS with rudder	230	31.6	10.8	0.1803	Low	7.33×10^6	1.39×10^9	1.281	14
					Design	1.26×10^7	2.39×10^9	2.196	24

3 Grid Dependence Study

Grid dependence studies have been performed for KVLCC2 and KCS hulls at two speeds and two grid configurations (with rudder and without rudder). Each grid dependence study has been performed with 5 geometrically similar grids. The finest grid is named as g1 while the coarsest grid denoted as g5. Considering the sensitivity of frictional resistance coefficient to the first layer thickness as highlighted in Korkmaz et al. (2019), average y^+ values are kept below the recommended value of 0.4 which was observed from the flat plate simulations.

All CFD calculations have been performed in double precision in order to eliminate the round-off errors. The iterative uncertainties have been determined from the standard deviation of the force in percent of the average force over the last 10% iterations. Iterative uncertainty for C_F and C_{PV} was kept below 0.01% and 0.15% for all simulations in model scale. Hence, it is assumed that the numerical errors are dominated by the discretization errors and both iterative errors and round-off errors are neglected.

There has been issues with the grids of the KCS hull around and behind the bulb. Close inspection has shown that the first layer thickness was varying irregularly due to difficulties of grid generation around the large protruding bulb at the forebody. Unfortunately, the issue hasn't been resolved completely but only a slight improvement was possible. The grid dependence analysis has shown that the calculated resistance components varied unexpectedly due to the meshing issue. Even though the variations were very limited (for example maximum variation of C_V is approximately 0.4% between 5 geometrically similar grids), it still caused rather high numerical uncertainties in bare hull cases. On the other hand, when the KCS hull is appended with rudder, numerical uncertainties are dropped significantly as presented in Table 2. In contrast to KCS hull, the simulations with KVLCC2 indicates similar uncertainty levels for different speed, turbulence model and existence of the rudder. The $k-\omega$ SST model gave slightly lower uncertainties compared to EASM. As it was the case for the KCS hull, existence of rudder reduced the uncertainties. The numerical uncertainties for KVLCC2 with rudder are presented in Table 2. Below 1% uncertainty was only achieved when the rudder was included in the simulations.

Table 2: Numerical uncertainties of KVLCC2 and KCS hulls, both with rudder and EASM turbulence model

KVLCC2						**KCS**					
$U_{SN}\%S$	g1	g2	g3	g4	g5	$U_{SN}\%S$	g1	g2	g3	g4	g5
C_F	1,3%	1,7%	2,3%	3,2%	4,8%	C_F	1,7%	1,8%	2,3%	3,0%	4,5%
C_{PV}	0,5%	1,6%	0,9%	1,2%	3,1%	C_{PV}	14,0%	17,0%	19,1%	24,7%	34,1%
C_V	0,8%	1,0%	1,0%	1,3%	1,4%	C_V	0,20 %	0,31 %	0,34 %	0,65 %	0,48 %

The first cell size have been varied with KCS and KVLCC2 hulls. The calculated C_F and C_V varies only marginally with the first cell size variation. It is significant to note that the maximum difference of C_F is around 0.1% at KCS hull case. The grid density of KCS hull g1 corresponds to g5 of the numerical flat plate investigations explained in Korkmaz et al. (2019). Such y+ variation caused 0.5% difference in C_F which is significantly larger than of the hull. Therefore it can be concluded that the effect of y^+ variation with a hull from is smaller than the flat plate case.

4 Sensitivity of form factor for varying loading conditions (different draughts and trims)

The loading condition varies during the operation of the ship. Typically, design and ballast loading conditions are tested in towing tanks. However, sea trials are often performed in ballast condition and sea trial at design condition is calculated via an extrapolation. Since the extrapolation is based on the model tests, it is critical to have the correct form factors. Due to the modern forebody designs or bows with bulbs, Prohaska method for obtaining the form factor at ballast condition is often not easy because of the significant wave patterns even at low Froude numbers. The same issue is also common at the design or other loading conditions. Therefore, CFD based form factor has potential improve the form factor determination. In this case, the first question is whether to perform the double model simulation with dynamic sinkage and trim or draught and trim at rest. The loading condition variation has also been suggested by Raven et al. (2009) as a solution to the large protruding bulbs for CFD based methods since the flow is accelerated or in some cases separated around the bulb. It is suggested that if the bulb the submerged more by trimming the hull (bow down) this issue can be prevented. The other issue of the form factor determination is the large submerged transoms which causes large separations behind the ship wake. It is worth to remember that the assumption of Hughes (1954) that form factor is the same in model and full scale is only valid if there is no flow separation. In order to reduce or eliminate the effect of a large submerged transom, the loading condition can be altered with reduced draught.

The loading condition (sinkage&trim) variation has been applied to KVLCC2 and KCS hulls. The form factor has been calculated based on the ITTC57 line and full scale viscous resistance (C_{V_S}) is calculated using the Eq. (1). As presented in Table 3, KVLCC2 and KCS hulls differ 0.24% and 0.10% in C_{V_S} between dynamic sinkage&trim and the draught&trim at rest for the design speed of each hull. This difference is significantly smaller for the lower speeds since the dynamic sinkage and trim is smaller compared to higher speeds. The trim variation is also applied to both hull forms in a way that the draught at the aft perpendicular is equal to the draught at rest (the pivot point) and the hull is trimmed bow up (- sign) or bow down (+ sign). The variation of C_{V_S} due to trim is shown as percentage with respect to the draught&trim at rest and presented in Table 3. Both hull forms indicated that form factor would increase when the hull is trimmed bow down (bow is submerged more) and vice versa for the bow down condition. Having in mind the slight variation in the grids between the trimmed hulls compared to dynamic sinkage and trim, it should be noted that the variation in C_{V_S} due to trim is smaller than the numerical uncertainties of each hull presented in Table 2.

Table 3: Form factor and viscous resistance variations as a result of different loading condition variation with EASM model, g2 with rudder at model scale design speed

KVLCC2					KCS			
Trim	Sinkage	k	C_{V_S}		Trim	Sinkage	k	C_{V_S}
dynamic	dynamic	0,230	0,24 %		dynamic	dynamic	0,106	0,10 %
0°	rest	0,227	ref.		0°	rest	0,105	ref.
0°	-2.5%	0,222	-0,37 %		0°	-2.5%	0,106	0,11 %
0°	2.5%	0,233	0,48 %		0°	2.5%	0,099	-0,55 %
0,25°	rest	0,233	0,46 %		0,25°	rest	0,107	0,19 %
-0,25°	rest	0,221	-0,49 %		-0,25°	rest	0,104	-0,04 %

Increasing the sinkage (with zero trim) for the KVLCC2 hull raises the form factor as expected since the transom is submerged even more compared to the original draught. Similarly, the form factor is decreasing with decreasing draught for the KVLCC2 hull. However, KCS hull indicated opposite trends for the sinkage variation compared to KCS hull. It should be noted that the transom of the KCS hull is not submerged even when the draught is increased 2.5%. On the other hand, the large part of the stern overhang is submerged when the draught is increased since buttocks are rather flat (a common feature for the container ships). As a result of large change in the submerged part of the aftbody due to increased draught, the C_{V_S} change is rather larger than other loading variations applied to the KCS hull.

5 Sensitivity of form factor for varying grid distributions

In addition to the grid dependence studies, several other grid setups have also been tested. The aim of this analysis is to determine the best grid distribution but also to figure out which grid distribution is not acceptable for the purpose of form factor determination. For this exercise, *g2* and *g5* of the grid dependence study has been selected as a starting point. The number of cells and longitudinal grid distribution of g2 has been selected based on the previous experiences. The coarsest grid g5 has only 1.69×10^6 cells. The new grid distributions are created by decreasing the number of cells in one region at a time and keeping all other regions the same. The flow domain and hull is divided into different regions longitudinally as can be seen in Figure 1. In Table 4, each grid is distinguished by it's parent grid (g2 or g5) and the modified region where the number of cells are changed. As an example, g2 grid with coarse bow and medium bow modification has 1/3 (35 cells) and 2/3 (70 cells) of number of cells in longitudinal direction at the bow region (see Figure 1) compared to original g2 grid (105 cells), respectively.

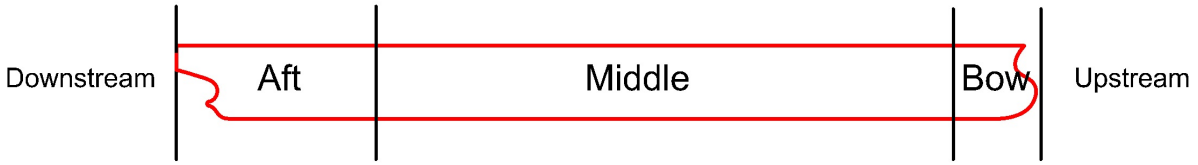

Fig. 1: Longitudinal divisions for grid generation

In Table 4, calculated form factors based ITTC57 line and extrapolated C_{V_S} values of KVLCC2 are presented for EASM and $k-\omega$ SST turbulence models. The coarsest grid with original grid distribution, g5, provides remarkably close C_{V_S} prediction (0.53% smaller) compared to g2 grid. As expected, the grids based on the parent grid of g2 is much less sensitive than g5. However, grids with coarser aft modification is more sensitive than coarser bow. The from factor obtained from the coarse aft grid based on the g5 is abnormally high for both turbulence models. It should be noted that this grid has only 20 cells in the longitudinal direction from aft shoulder to transom. The absolute values of C_{V_S} values are different but the relative changes between the grids are almost the same for both turbulence models.

Table 4: Grid variation, rudder appended at model scale design speed

Parent grid	Modification	Cells	EASM		$k-\omega$ SST	
			k	C_{V_S}	k	C_{V_S}
g2	Original	$8{,}39\times10^6$	0,227	ref.	0,245	ref.
g2	Coarse Bow	$7{,}66\times10^6$	0,233	0,49 %	0,251	0,45 %
g2	Medium Bow	$8{,}02\times10^6$	0,228	0,07 %	0,248	0,18 %
g2	Coarse Aft	$7{,}66\times10^6$	0,236	0,76 %	0,254	0,70 %
g2	Medium Aft	$8{,}02\times10^6$	0,228	0,07 %	0,248	0,18 %
g5	Original	$1{,}69\times10^6$	0,220	-0,53 %	0,240	-0,47 %
g5	Coarse Bow	$1{,}55\times10^6$	0,233	0,49 %	0,250	0,36 %
g5	Medium Bow	$1{,}62\times10^6$	0,223	-0,34 %	0,241	-0,34 %
g5	Coarse Aft	$1{,}55\times10^6$	0,318	7,42 %	0,337	7,32 %
g5	Medium Aft	$1{,}62\times10^6$	0,223	-0,34 %	0,241	-0,34 %

6 Speed dependency of form factor

The scale effects on the form factor has been previously mentioned. In this section, scale effects have been demonstrated by varying the speed of the KVLCC2 and KCS hulls. Since the simulations are performed as double model, the form factors obtained from different speeds should be the same since form factor should be independent of the Reynolds number. The form factor and the full scale viscous resistance (extrapolated) figures are presented in Table 5 and Table 6 for KCS and KVLCC2, respectively. The

same grid density, g2, were used and both hulls are appended with rudders. The form factor and the C_{V_S} values are calculated using both ITTC57 line and numerical friction lines of the corresponding turbulence model used for the calculations. The numerical friction lines for EASM and $k-\omega$ SST turbulence model were derived using SHIPFLOW and used for this study as recommended in Korkmaz et al. (2019). As can be seen in Table 5 and Table 6, the form factors based on the ITTC57 line differs significantly with the varying speed for both hulls and turbulence models. However, when the numerical friction lines are applied, form factors are almost the same at different speeds for the same turbulence model. The form factors differ for the different turbulence models because calculated C_{V_M} is different and also the numerical friction line for EASM and $k-\omega$ SST models are different when numerical friction line is used. However, the difference between extrapolated C_{V_S} values from different turbulent models are significantly smaller when numerical friction lines are applied instead of the ITTC57 line. In Table 7, results of the full scale simulations are presented for the KCS hull. It should be noted that when ITTC57 line is used, extrapolated C_{V_S} values are significantly smaller compared to computed C_{V_S} values.

Table 5: Calculated form factor and extrapolated C_{V_M} values of KCS with rudder

		ITTC57 line			numerical friction line		
Turbulence model	Speed	k	C_{V_S}(14kts)	C_{V_S}(24kts)	k	C_{V_S}(14kts)	C_{V_S}(24kts)
EASM	design	0,106	$1{,}626\times10^{-3}$	$1{,}524\times10^{-3}$	0,169	$1{,}740\times10^{-3}$	$1{,}644\times10^{-3}$
EASM	low	0,088	$1{,}600\times10^{-3}$	$1{,}499\times10^{-3}$	0,169	$1{,}740\times10^{-3}$	$1{,}643\times10^{-3}$
$k-\omega$ SST	design	0,132	$1{,}664\times10^{-3}$	$1{,}559\times10^{-3}$	0,159	$1{,}754\times10^{-3}$	$1{,}649\times10^{-3}$
$k-\omega$ SST	low	0,117	$1{,}642\times10^{-3}$	$1{,}539\times10^{-3}$	0,158	$1{,}753\times10^{-3}$	$1{,}648\times10^{-3}$

Table 6: Calculated form factor and extrapolated C_{V_M} values of KVLCC2 with rudder

		ITTC57 line			numerical friction line		
Turbulence model	Speed	k	C_{V_S}(13kts)	C_{V_S}(15.5kts)	k	C_{V_S}(13kts)	C_{V_S}(15.5kts)
EASM	design	0,230	$1{,}752\times10^{-3}$	$1{,}717\times10^{-3}$	0,340	$1{,}940\times10^{-3}$	$1{,}905\times10^{-3}$
EASM	low	0,219	$1{,}737\times10^{-3}$	$1{,}701\times10^{-3}$	0,337	$1{,}936\times10^{-3}$	$1{,}901\times10^{-3}$
$k-\omega$ SST	design	0,249	$1{,}779\times10^{-3}$	$1{,}743\times10^{-3}$	0,308	$1{,}923\times10^{-3}$	$1{,}885\times10^{-3}$
$k-\omega$ SST	low	0,238	$1{,}764\times10^{-3}$	$1{,}728\times10^{-3}$	0,304	$1{,}917\times10^{-3}$	$1{,}880\times10^{-3}$

Table 7: Full scale simulations of KCS

speed	EASM	$k-\omega$ SST
C_{V_S}(14kts)	1.747×10^{-3}	1.772×10^{-3}
C_{V_S}(24kts)	1.603×10^{-3}	1.665×10^{-3}

7 Conclusions

In this study, CFD based form factor determination method have been investigated by analyzing the calculations performed on KVLCC2 and KCS hulls. The following observations have been made:

- Grid dependence studies indicated that numerical uncertainties around 1% is achievable with KVLCC2 hull regardless of existence of rudder and the choice of turbulence model (EASM and $k-\omega$ SST). On the other hand, there has been meshing issues with KCS at the forebody due to large protruding bulb. The numerical uncertainties around 1% was only possible when the rudder appended to the KCS hull.

- Frictional resistance component was less sensitive to the first layer thickness with KCS and KVLCC2 hulls compared to flat plate simulations.

- The loading condition (sinkage&trim) variation had limited effect on the calculated form factor for both KCS and KVLCC2 hulls. The difference in the extrapolated C_{V_S} values due to varying sinkage&trim were often smaller than the numerical uncertainties.

- Different grid density distributions have been simulated in order to find out which grid density is acceptable and which grids should be avoided. The sensitivity of form factor to the grid density at the aft body is bigger than the forebody. It can be argued that unless the grid resolution at the aftbody is very coarse, sensitivity of form factor to the grid resolution at the other parts of the hull is rather low.

- The scale effects on form factor have been one of the most important discussion topic. It has been showed that when ITTC57 line is used, the scale effects are in-avoidable. However, when the numerical friction line that of the same CFD code and same turbulence model is applied scale effects are reduced significantly. The computations with EASM turbulence model with the numerical friction line of the same turbulence model eliminated the scale effects almost completely.

- The EASM and $k-\omega$ SST turbulence models gives different form factors regardless of the friction line used. However, when the numerical friction line is used, the variation of the extrapolated C_{V_S} values between turbulence models are reduced compared to ITTC57 line.

- The C_{V_S} obtained from the full scale simulations with KCS is significantly closer to the extrapolated C_{V_S} when the numerical friction lines are used.

Acknowledgements

This project has been funded by *Vinnova* and the computational resources were provided by the Chalmers Center for Computational Science and Engineering (C3SE).

References

A. García-Gómez (2000). On the Form Factor Scale Effect. *Ocean Engineering*, **Vol. 26**, p.97-109.

C. W. Prohaska (1966). A Simple Method for the Evaluation of the Form Factor and Low Speed Wave Resistance. *Proceeding of 11th ITTC*.

C.W.B. Grigson (1999). A planar algorithm and its use in analysing hull resistance. *Trans. RINA*, **Vol. 142** p.76-115.

G. Hughes (1954). Friction and Form Resistance in Turbulent Flow, and a Proposed Formulation for Use in Model and Ship Correlation. *Trans. RINA*, **Vol. 96**, p.314-376.

H. C. Raven, A. van der Ploeg, A.R. Starke and L. Eça (2009). Towards a CFD-based prediction of ship performance — progress in predicting full-scale resistance and scale effects. *International Journal of Maritime Engineering*, **Vol. 135**.

K.B. Korkmaz, S. Werner, R. Bensow (2019). *Numerical Friction Lines For CFD Based Form Factor Determination. VIII International Conference on Computational Methods in Marine Engineering (Marine 2019).*

L. Eça and M. Hoekstra (2014). A Procedure for the Estimation of the Numerical Uncertainty of CFD Calculations Based on Grid Refinement Studies. *Journal of Computational Physics*, **Vol. 262** p.104-130.

N. Toki (2008). Investigation on Correlation Lines through the Analyses of Geosim Model Test Results. *Journal of the Japan Society of Naval Architects and Ocean Engineers*, **Vol. 8**, p.71-79.

Proceedings of the 8th ITTC (1957).

S.-H. Van, H. Ahn, Y.-Y Lee, C. Kim, S. Hwang, J. Kim, K.-S Kim, and I.-R Park (2011). Resistance Characteristics and Form Factor Evaluation for Geosim Models of KVLCC2 and KCS. *Advanced Model Measurement Technology for EU Maritime Industry*.

T. Katsui, H. Asai, Y. Himeno and Y. Tahara, (2005). The Proposal of a New Friction Line. *Fifth Osaka Colloquium on Advanced CFD Applications to Ship Flow and Hull Form Design, Osaka, Japan*.

Z.-z. Wang, Y. Xiong, L.-p Shi and Z,-h Liu (2015). A Numerical Flat Plate Friction Line and Its Application. *Journal of Hydrodynamics*, **Vol. 23**(3) p.383-393.